Y3.N21/5:6/1528

GOVT. DOC.

NACA TN No. 1528

NATIONAL ADVISORY COMMITTEE FOR AERONAUTICS

TECHNICAL NOTE

No. 1528

TESTS OF A 45° SWEPTBACK-WING MODEL IN THE LANGLEY GUST TUNNEL

By Harold B. Pierce

Langley Memorial Aeronautical Laboratory
Langley Field, Va.

Washington
February 1948

~~CONN. STATE LIBRARY~~

MAR 1 1948

BUSINESS, SCIENCE
& TECHNOLOGY DEP'T.

NATIONAL ADVISORY COMMITTEE FOR AERONAUTICS

TECHNICAL NOTE NO. 1528

TESTS OF A 45° SWEPTBACK-WING MODEL IN THE LANGLEY GUST TUNNEL

By Harold B. Pierce

SUMMARY

A series of tests of a 45° sweptback-wing model with and without fuselage and of an equivalent straight-wing model were conducted in the Langley gust tunnel to provide information on some of the problems encountered in the prediction of gust loads for airplanes incorporating swept wings. A comparison of test results with calculated results indicated that the maximum acceleration increment resulting from the penetration of a gust by a sweptback-wing airplane may be assumed to be dependent on the slope of the lift curve of the equivalent straight wing multiplied by the cosine of the angle of sweep, rather than on the steady-flow slope of the lift curve. In addition, it appeared that the maximum acceleration increment also depends on the effect on the unsteady-lift function of the gradual penetration of the sweptback wing into the gust. A comparison of the maximum acceleration increments obtained for the swept-wing model with those obtained for the straight-wing model indicated that, although the airplane with a swept wing would show positive pitching motion, it would undergo a much lower acceleration increment than the same airplane with the equivalent straight wing.

INTRODUCTION

One of the problems associated with improving high-speed flight by the use of wings with large angles of sweep is the prediction of gust load factors. Some of the elements to be considered in the calculation of gust loads for these wing configurations include: (a) the prediction of a slope of the wing-lift curve, (b) the determination of the effects of the gradual penetration of a swept wing into a gust, and (c) the possible increase in fuselage-interference effects such as described in reference 1. Other elements to be considered are the effects of compressibility and of wing flexibility. The problems cited concerning the slope of the wing-lift curve, the penetration effect, and the fuselage-interference effect depend primarily on the wing configuration alone and are important in setting the magnitudes of the gust load factors for swept wings relative to those for the conventional straight-wing airplane on which much information is already available. On the other hand, the

problems resulting from compressibility are common to all wing configurations, whereas the problem resulting from wing flexibility that is peculiar to the swept-wing configuration, namely, wing twist due to bending, depends to a great extent on the structural properties of the individual design.

As a starting point, analytical studies together with suitable tests were made in the Langley gust tunnel in order to provide information pertinent to these problems exclusive of compressibility and flexibility effects. This paper presents the results of gust-tunnel tests of a model having a rigid wing with the half-chord line swept back 45° and the results of tests of an equivalent model having 0° sweep. The test results are compared with the results of analytical studies, and some information on the determination of a wing-lift-curve slope and on the entry-interference and fuselage-interference effects is obtained.

APPARATUS

Photographs of the skeleton models used in the tests are shown as figures 1 and 2, and plan-view line drawings are shown as figures 3 and 4. A removable fuselage was provided for the sweptback-wing model (fig. 5 and dashed lines in fig. 3) so that tests to determine the effects of fuselage interference could be made with the same model. The characteristics of the models and the test conditions are listed in table I. In order to provide space for batteries and the accelerometer in the wings of the models, the center sections had smooth bulges which projected from the top and bottom surfaces and which about doubled the wing thicknesses.

The wing of the straight-wing model (fig. 4) had 0° sweep of the straight line through the half-chord points and an NACA 0012 airfoil section perpendicular to this line. The wing of the swept-wing model was derived from that of the straight-wing model, or from the equivalent straight wing as it will be hereinafter called, by rotating the straight wing about the half-chord point at the plane of symmetry so that the constant length half-chord line moved back through an angle of 45°. The wing tip was modified to the form indicated in figure 3.

Force tests were made in the Langley free-flight tunnel of the equivalent straight-wing model and of the sweptback-wing model without fuselage, and the results are shown in figure 6. The slopes of the lift curves of the models as determined by these tests are included in table I.

The present Langley gust tunnel is the same in principle as the gust tunnel described in reference 1 and utilizes like instrumentation and techniques. The capacity of the gust-tunnel equipment now used is such that 6-foot-span models can be flown up to speeds of 100 miles an hour

through gusts with velocities up to 20 feet per second. The gust or jet of air supplied by the Langley gust tunnel is 8 feet wide and 14 feet long and, at the present time, is screened with special wire-mesh screening to insure a reasonable low level of turbulence.

TESTS

Tests of the sweptback-wing model consisted of nine flights of the model with and eight without the fuselage through the sharp-edge gust shown in figure 7(a). Tests of the equivalent straight-wing model consisted of 10 flights of the model through the sharp-edge gust shown in figure 7(b). The tests were all made for a forward speed of 60 miles per hour and a gust velocity of approximately 10 feet per second. Measurements of the forward speed, gust velocity, normal-acceleration increments, and pitch-angle increment were made during each flight.

RESULTS

Records for all flights were evaluated to obtain histories of the normal-acceleration increment and pitch-angle increment during traverse of the gust. Representative histories of results for tests in a sharp-edge gust of the sweptback-wing model with and without fuselage and for tests of the equivalent straight-wing model without a fuselage are shown in figure 8(a). The results are plotted against the position of the airplane center of gravity in terms of mean-aerodynamic-chord lengths of travel from the leading edge of the Langley gust-tunnel test section.

Histories of events for the sweptback-wing model penetrating a gust with a gradient distance of 9 chords were obtained by building up by superposition the histories obtained in the sharp-edge gust under the assumption that the sharp-edge gust could be considered to be a "unit-jump" type gust. The gradient distance of 9 chords was the maximum that could be obtained, since the method is limited by the extent of the original histories. For the purpose of determining the maximum value of the built-up curves, the histories were extrapolated an extra chord length. For comparative purposes, the histories of events in the sharp-edge gust for the equivalent straight-wing model were also built up to represent the response of the model in a gust of 9-chord gradient distance. Sample histories of responses to a gust with a gradient distance of 9 chords are shown in figure 8(b) for the equivalent straight-wing model and for the sweptback-wing model with and without fuselage.

The maximum acceleration increments Δn_{max} obtained from tests of the

45° sweptback-wing models in the sharp-edge gust and those obtained from the building up of the results to represent the response to a gust of 9-chord gradient distance are presented in table II. Since the model weights were different (table I) and each flight was made at slightly different values of forward velocity and gust velocity, the maximum acceleration increments were all corrected to a model weight of 9.25 pounds, a forward velocity of 60 miles per hour, and a gust velocity of 10 feet per second on the assumption that they are inversely proportional to the model weight and directly proportional to forward speed and gust velocity (reference 1).

PRECISION

The measured quantities are estimated to be accurate within the following limits for any test or run:

Acceleration increment, Δn, g units	±0.05
Forward velocity, feet per second	±0.5
Gust velocity, feet per second	±0.1
Pitch-angle increment, degrees	±0.1

In any given flight, small variations in the launching speed or attitude of the model tend to produce errors in the acceleration increment which are a function of the pitching motion of the model. In most cases the tendency is to introduce an upward pitching velocity, which may remain constant throughout the traverse (reference 2). It is not possible at present to eliminate such errors by means of corrections to the data. Consideration of all factors involved, however, indicates that the results from repeat flights should have a dispersion of not more than ±0.05 g for a sharp-edge gust. Similar considerations indicate that the dispersion should not exceed ±0.1 g when the responses to the sharp-edge gust are built up to represent the responses to a gust with a gradient distance of 9 chords.

ANALYSIS

Calculations to predict the responses of the equivalent straight-wing model and of the 45° sweptback-wing model without fuselage to the test gust were made under the following assumptions:

(1) The pitching motion is neglected.

(2) The wings are rigid.

(3) Only the load increment on the wing is considered.

The following equation, derived from equation (1) of reference 2, may then be considered to determine the acceleration increment of an airplane in a gust at any point s_1:

$$\Delta n = \frac{\rho m V S}{2W} \int_0^{s_1} C_{L_g}\left(s_1 - s\right) \frac{dU}{ds}\, ds - \frac{\rho m S c g}{2W} \int_0^{s_1} C_{L_\alpha}\left(s_1 - s\right) \Delta n(s)\, ds \quad (1)$$

where

Δn	acceleration increment, g units
ρ	mass density of air, slugs per cubic foot
m	slope of wing-lift curve, per radian
V	forward velocity, feet per second
S	wing area, square feet
W	weight of model, pounds
s	distance penetrated into gust by foremost point of leading edge of wing, chords
s_1	distance penetrated into gust by foremost point of leading edge of wing at which acceleration increment is to be determined, chords
$\Delta n(s)$	history of acceleration increment expressed as a function of s
c	wing chord length, feet
g	acceleration due to gravity, feet per second^2
U	gust velocity, feet per second
$C_{L_g}\left(s_1 - s\right)$	unsteady-lift function for an airfoil penetrating a sharp-edge gust expressed as a function of $s_1 - s$
$C_{L_\alpha}\left(s_1 - s\right)$	unsteady-lift function for a sudden change of angle of attack over entire wing expressed as a function of $s_1 - s$

For the purpose of this paper, C_{L_g} and C_{L_α} are the ratios of the lift coefficient at any distance s to the lift coefficient after an infinite distance has been traversed (steady flow).

In the solution for the response to the sharp-edge gust, equation (1) may be reduced as follows:

$$\Delta n = \frac{\rho mUVS}{2W}\left[C_{L_g}(s)\right]_{s_1} - \frac{\rho mSV}{2W}\int_0^{s_1} C_{L_\alpha}\left(s_1 - s\right)\frac{dw}{ds}\,ds \qquad (2)$$

where $C_{L_g}(s)$ is the unsteady lift function for an airfoil penetrating a sharp-edge gust expressed as a function of s; $\left[C_{L_g}(s)\right]_{s_1}$ is the value of the function at s_1; and w is successively, in the iteration for solution by the graphical method given in reference 3, the history of the vertical velocity determined from the history of the first term of equation (2) and then from the histories of Δn until convergence.

In accordance with the results of past analyses, such as in references 1 and 2, unsteady-lift functions for two-dimensional flow (infinite aspect ratio) were used and the neglect of the influence of the tip vortices was assumed to be accounted for by the use of the slope of the lift curve of the three-dimensional wing. In making the calculations, the slopes of the wing-lift curve determined by wind-tunnel tests were used for both models. In addition, calculations were made for the sweptback-wing model with the use of a slope of the lift curve determined by the so-called "cosine law," which is the process of multiplying the slope of the lift curve of the equivalent straight wing by the cosine of the angle of sweep (reference 4). The unsteady-lift functions C_{L_g} and C_{L_α} were derived from the functions for infinite aspect ratio given by Jones in reference 5, and these functions were used in the calculations for the equivalent straight-wing model. In the calculations for the sweptback-wing model, however, the function C_{L_g} was modified by strip theory to take into account the gradual penetration of the sweptback wing into the gust. The curves for C_{L_α} and C_{L_g} modified and unmodified are given in figure 9.

The maximum acceleration increments determined by equation (2) for the sharp-edge gust and those determined by building up by superposition for the gust of 9-chord gradient distance are included in table II for both slopes of the lift curve used.

For comparative purposes, results of calculations made by the method of reference 6 for the sharp-edge gusts and for the gusts with 9-chord gradient distances are also included in table II. The slope of the lift

curve used was derived by the cosine law. The equations of reference 6 are a solution of equation (1) of the present paper using an unmodified curve of C_{L_g}; and, in the case of gradient gusts, the additional assumption is made that the acceleration increment reaches a maximum value at the same time the gust reaches its maximum.

DISCUSSION

Examination of the test results given in figure 8 shows that appreciable pitching motion is present at the time of maximum acceleration increment for both the sharp-edge and 9-chord-gradient-distance gusts. In order that the comparison of the experimental data with the calculated data be valid, the effect of the pitching motion was removed from the experimental data of Δn_{max} shown in table II by use of an approximate correction such that

$$\Delta n_{max_0} = \Delta n_{max}\left(1 - \frac{\Delta\theta/57.3}{U/V}\right) \tag{3}$$

where Δn_{max_0} represents Δn_{max} reduced to zero pitch and $\Delta\theta$ is the pitch increment in degrees at the time of occurrence of Δn_{max}. This approximate correction factor has been shown to be applicable in the unpublished results of several series of tests made in the Langley gust tunnel. The resultant values of Δn_{max} reduced to zero pitch are given in table II.

When the experimental results reduced to zero pitching motion are compared with the calculated results in table II, good agreement between these results is noted in the case of the equivalent straight-wing model. The comparison for the sweptback-wing model shows that the best agreement with experiment is obtained with the results calculated by the method of this paper by the use of a lift-curve slope derived by the cosine law. The good agreement between calculated and experimental results for the equivalent straight-wing model indicates that, for this case, the slopes of the lift curve are about the same in both the steady-flow and unsteady-flow or gust conditions. For the sweptback-wing model, however, the slope of the lift curve in the unsteady-flow or gust condition appears to be about 20 percent higher than the measured slope in steady flow. It is believed that this difference can be ascribed to the behavior of the boundary layer in the unsteady-flow condition; but, at the present time, sufficient evidence to support this premise is not available.

The comparison in table II of the results of the calculation by the present method, which uses the modified curve of C_{L_g} of figure 9,

with the results of the calculations by the method of reference 6, which uses a curve of C_{L_g} similar to the unmodified curve in figure 9 (both methods using a lift-curve slope derived by the cosine law), indicates that the effect of the gradual penetration on the unsteady-lift function C_{L_g} should be taken into account in a calculation for gust loads on sweptback wings. The reduction of area under the curve of C_{L_g} caused by the modification for the penetration effect is, of course, the reason for the lower values of acceleration increment predicted by the method given in this paper.

The effect on the maximum acceleration increment of the addition of the fuselage to the sweptback-wing model appears to be negligible when the results are reduced to zero pitch (table II). It is probable that this condition is due to the fact that with the particular configuration used, the length of the fuselage is not a great deal different from the distance along the flight path from the leading edge of the wing center line to the trailing edge of the wing tip. For a normal straight-wing airplane, the chord length of the fuselage is three to four times that of the wing; and tests with and without a fuselage would probably show a difference in maximum acceleration increment.

The pitching motion of the two models is shown in figure 8 and the effect of the pitching motion on the measured acceleration increments is shown in table II. For the 45° sweptback-wing model, the positive pitching motion accounts for about a 10-percent increase in acceleration increment over the no-pitch motion when the small effects of the fuselage on the pitching motion are ignored. On the same basis, the positive pitching motion of the equivalent straight-wing model would account for about a 4-percent increase in acceleration increment over the no-pitch condition. If it is assumed that the equivalent straight-wing and the swept-wing models have the same stability characteristics, the effect on the total acceleration increment of the positive pitching motion of the sweptback-wing model appears to be some 6 percent greater than the similar effect for the equivalent straight-wing model. Such a trend might be expected from a general consideration of the effect of the gradual immersion of a sweptback wing in a gust as compared with the almost instantaneous immersion of the entire span of a straight wing. Although there were no comparable equivalent-straight-wing model tests to provide a basis for determining relative pitch effects, unpublished tests of a tailless model having a wing swept back 30° also showed a trend toward positive pitching motion and increased acceleration increments. On the basis of this limited information, then, it appears that airplanes having sweptback wings will exhibit a tendency toward positive pitching motion upon entry into a gust.

The comparison in table II of the observed acceleration increments for the equivalent straight-wing and the swept-wing models shows a

large reduction in acceleration increment in the same gust for the sweptback-wing model, which appears to result from the penetration effect on the curve of C_{L_g} combined with the reduction of the slope of the wing-lift curve by the rotation of the wing through the angle of sweep. It appears, then, that an airplane with a sweptback wing would have a much lower acceleration increment imposed on it from penetration of a gust than would the same airplane with an equivalent straight wing.

CONCLUDING REMARKS

Within the limits of the data, the excellent agreement in the no-pitch condition between the test results for a 45° sweptback-wing model and the results of the calculation by the method presented indicated that the maximum acceleration increment experienced in a gust by a sweptback-wing airplane depends on: (1) the slope of the lift curve of the equivalent straight-wing multiplied by the cosine of the angle of sweep rather than on the steady-flow slope of the lift curve and (2) the effect of the gradual penetration of the gust on the unsteady-lift function.

In addition, the results of the tests indicated that in a gust the acceleration increment of an airplane with a swept wing would be much less than that for the same airplane with an equivalent straight wing, even if the trend toward positive pitching motion that is indicated for airplanes having large angles of sweepback is considered.

Langley Memorial Aeronautical Laboratory
National Advisory Committee for Aeronautics
Langley Field, Va., October 8, 1947

REFERENCES

1. Donely, Philip: An Experimental Investigation of the Normal Acceleration of an Airplane Model in a Gust. NACA TN No. 706, 1939.

2. Donely, Philip, Pierce, Harold B., and Pepoon, Philip W.: Measurements and Analysis of the Motion of a Canard Airplane Model in Gusts. NACA TN No. 758, 1940.

3. Jones, Robert T.: Calculation of the Motion of an Airplane under the Influence of Irregular Disturbances. Jour. Aero. Sci., vol. 3, no. 12, Oct. 1936, pp. 419–425.

4. Letko, William, and Goodman, Alex: Preliminary Wind-Tunnel Investigation at Low Speed of Stability and Control Characteristics of Swept-Back Wings. NACA TN No. 1046, 1946.

5. Jones, Robert T.: The Unsteady Lift of a Wing of Finite Aspect Ratio. NACA Rep. No. 681, 1940.

6. Rhode, Richard V.: Gust Loads on Airplanes. SAE Jour., vol. 40, no. 3, March 1937, pp. 81–88.

TABLE I

CHARACTERISTICS OF MODELS AND TEST CONDITIONS

	Sweptback-wing model		Equivalent straight-wing model
	Without fuselage	With fuselage	
Weight, W, lb	9.25	9.75	9.875
Wing area, S, sq ft	6.05	6.05	6.00
Wing loading, W/S, lb/sq ft	1.53	1.61	1.64
Span, b, ft	4.25	4.25	6.00
Mean aerodynamic chord measured in plane parallel to plane of symmetry, $\bar{c}$, ft	1.4777	1.4777	1.037
Aspect ratio, b^2/S	2.99	2.99	6.00
Root chord, c_s, ft	1.90	1.90	1.33
Tip chord, c_t , ft	0.95	0.95	0.67
Taper ratio, c_t/c_s	0.5	0.5	0.5
Sweep angle of half-chord line, deg . .	45	45	0
Wing area intercepted by fuselage, percent gross wing area	0	15.8	0
Slope of lift curve determined by force tests, per radian	2.58	----	4.41
Slope of lift curve determined by multiplying lift-curve slope of equivalent straight wing by cosine of sweep angle, per radian	3.12	3.12	4.41
Center-of-gravity position, percent $\bar{c}$.	32.45	32.45	31.25
Gust velocity, U, fps	10	10	10
Forward velocity, V, mph	60	60	60

TABLE II

COMPARISON OF EXPERIMENTAL AND CALCULATED

MAXIMUM ACCELERATION INCREMENTS

Gradient distance (chords)	Experimental Δn_{max} (g units)		Experimental Δn_{max} reduced to zero pitch (g units)		Calculated Δn_{max} by present method (g units)		Calculated Δn_{max} from reference 6 (g units)
	Without fuselage	With fuselage	Without fuselage	With fuselage	Cosine-law slope	Measured steady-flow slope	
Equivalent straight-wing model							
0	2.11	---	2.03	---	1.96	1.96	2.00
9	1.73	---	1.67	---	1.65	1.65	1.72
45° sweptback-wing model							
0	1.48	1.43	1.34	1.34	1.35	1.12	1.41
9	1.13	1.12	1.03	1.03	1.05	.87	1.22

NACA

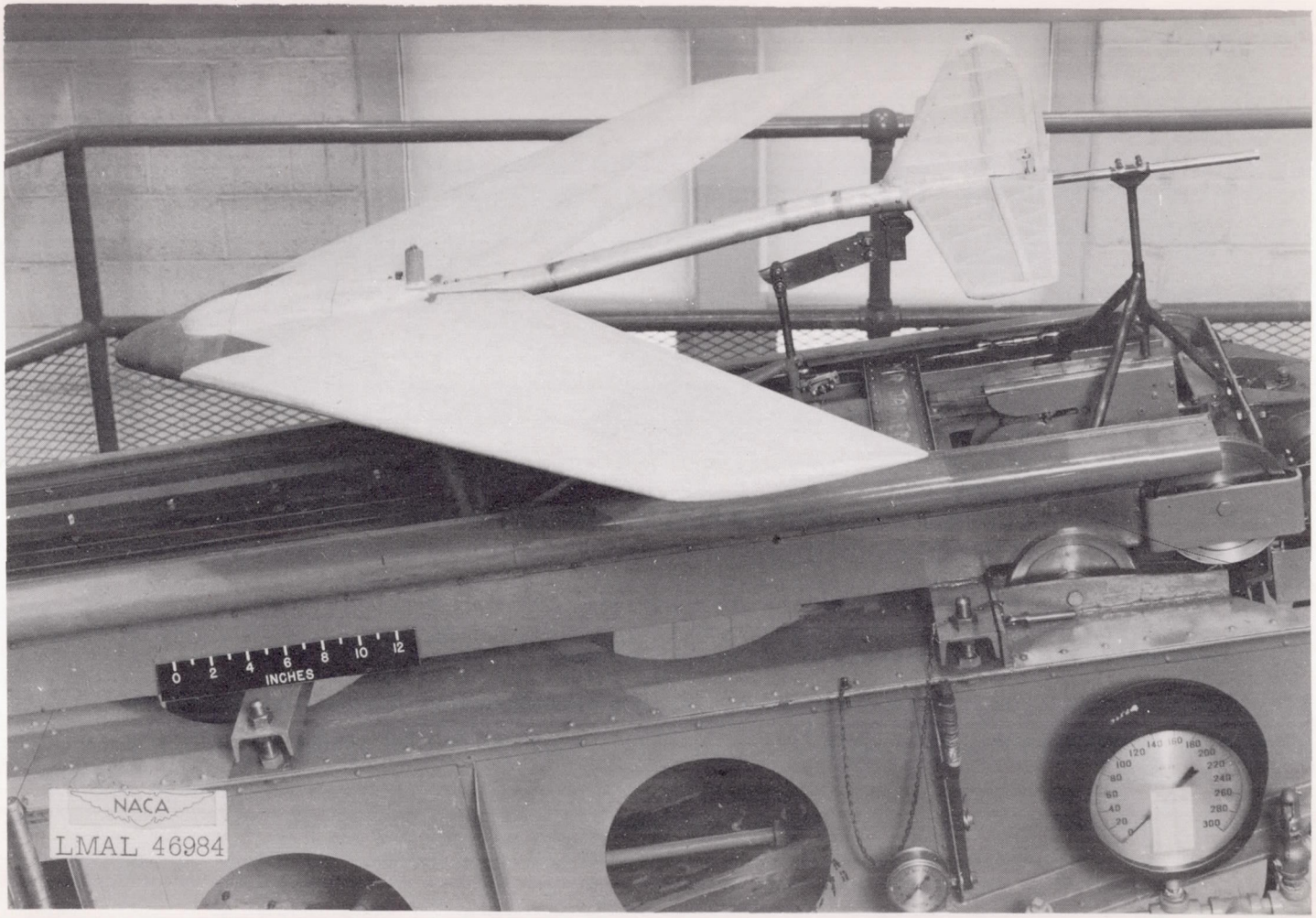

Figure 1.- Sweptback-wing model without fuselage.

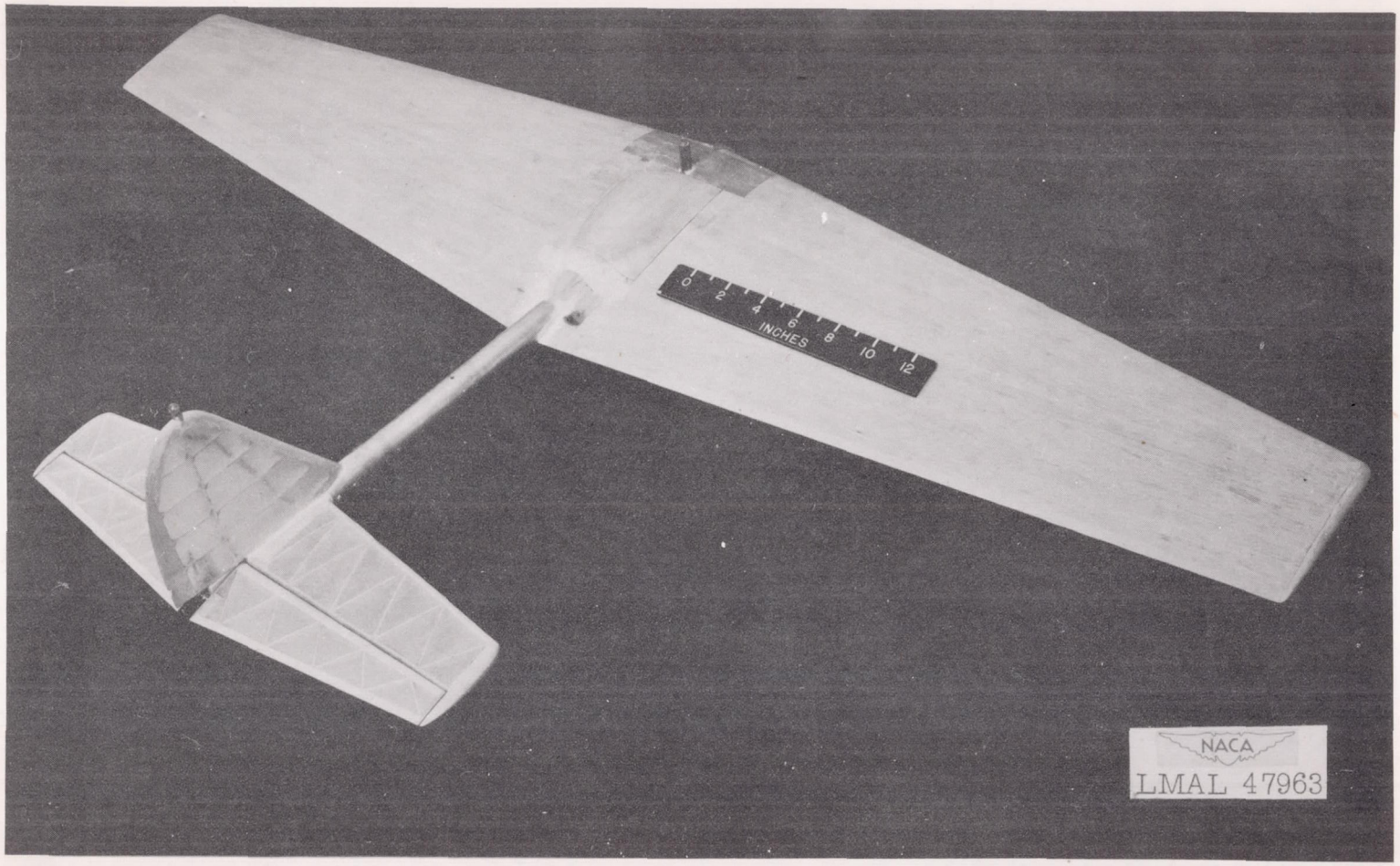

Figure 2.- Equivalent straight-wing model.

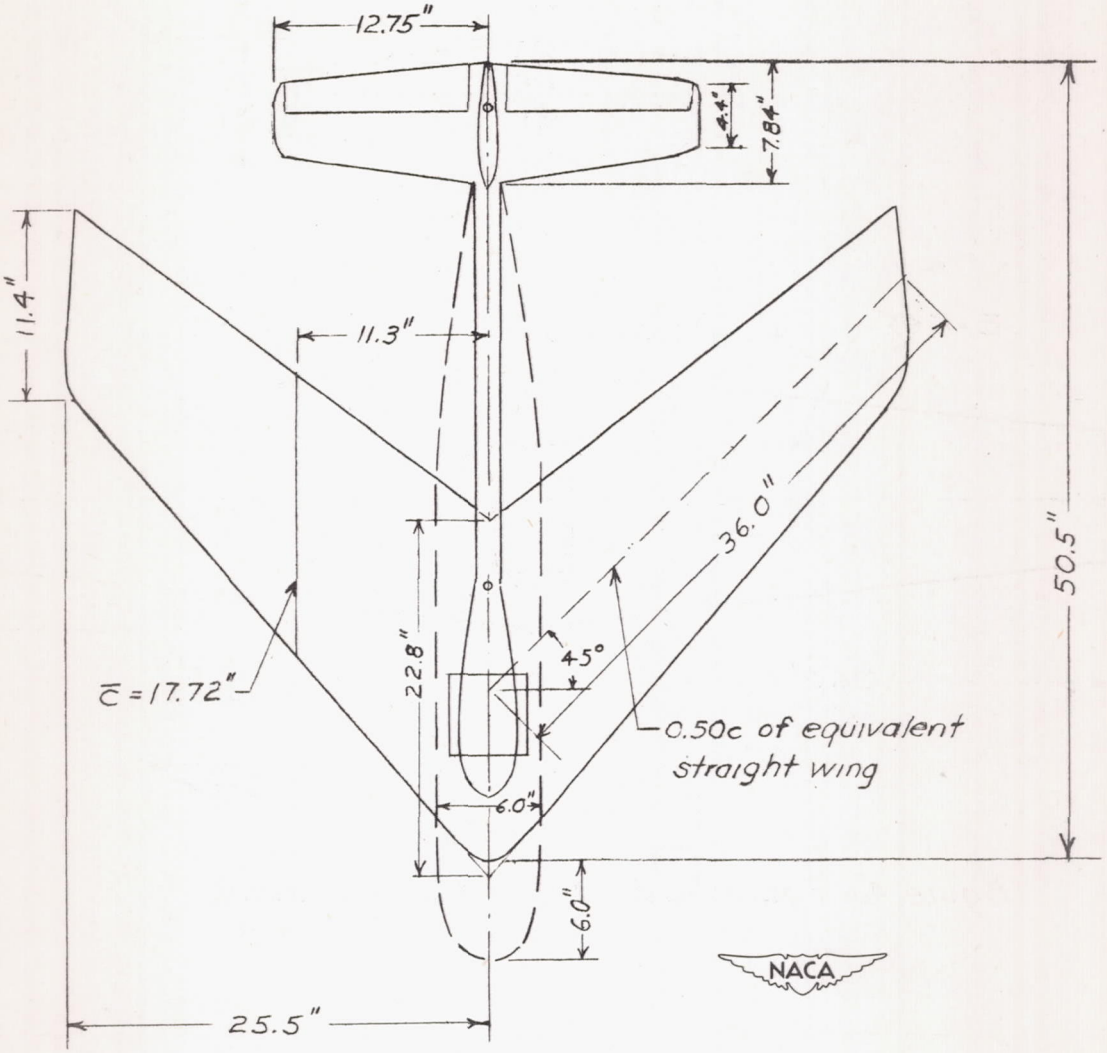

Figure 3.– 45° sweptback wing model.

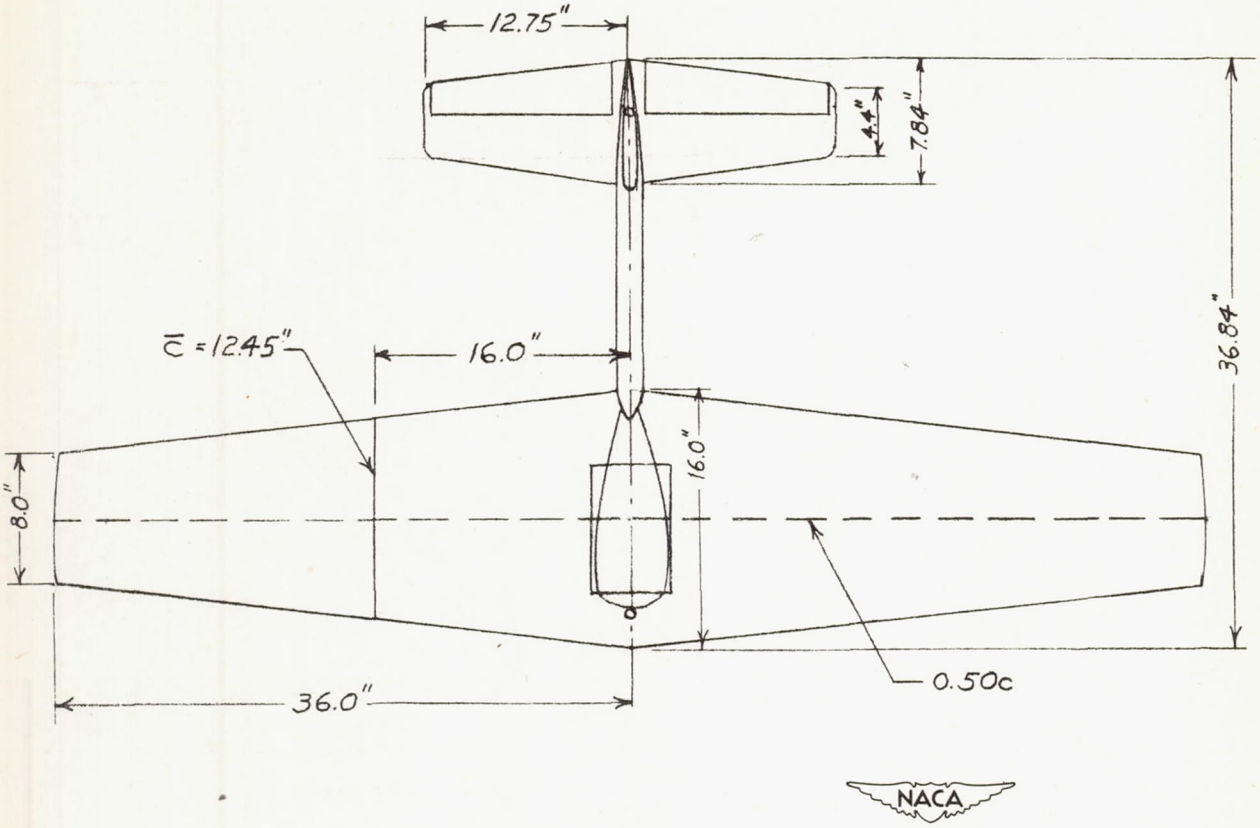

Figure 4.- Equivalent straight-wing model.

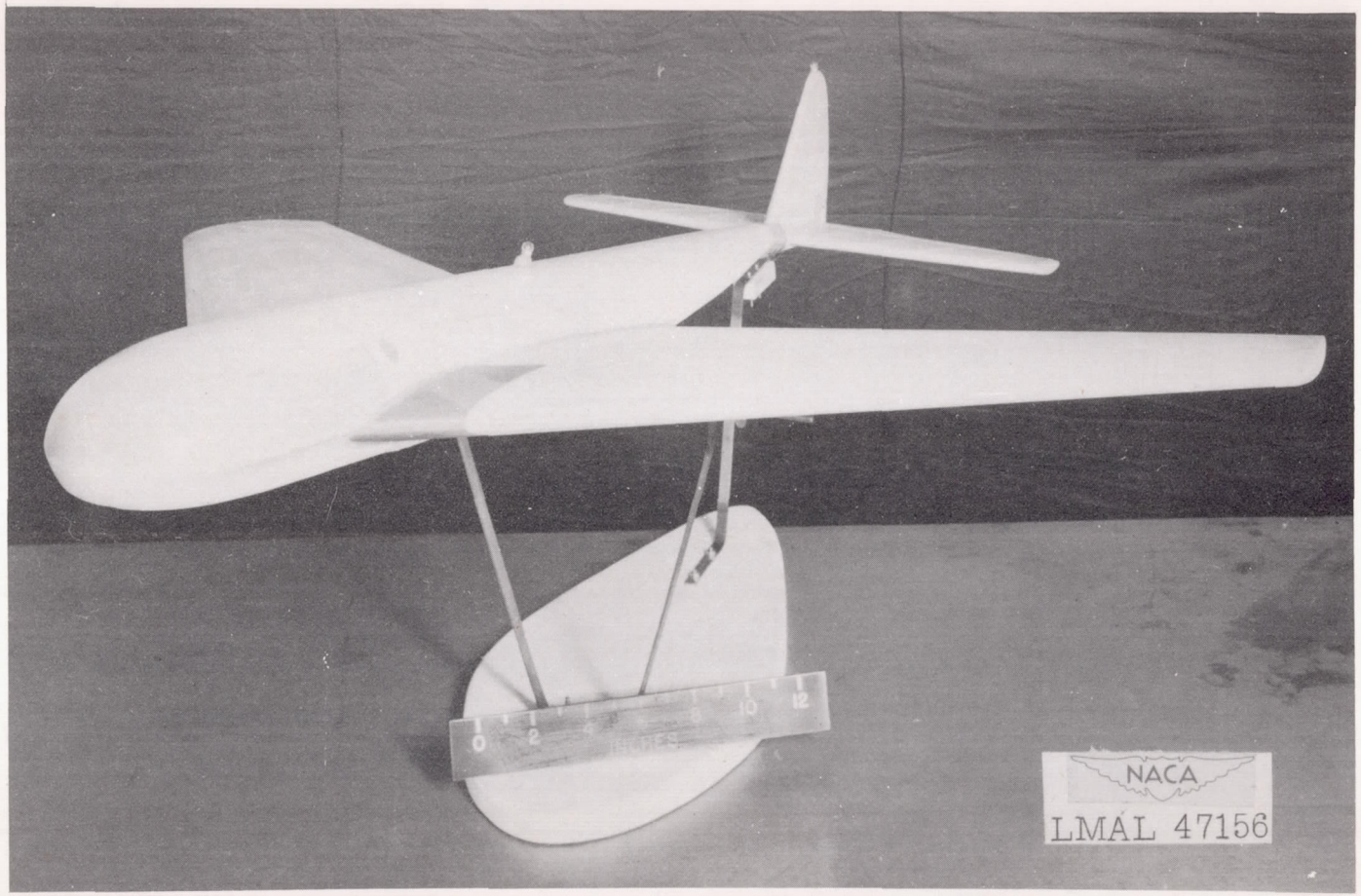

Figure 5.- Sweptback-wing model with fuselage.

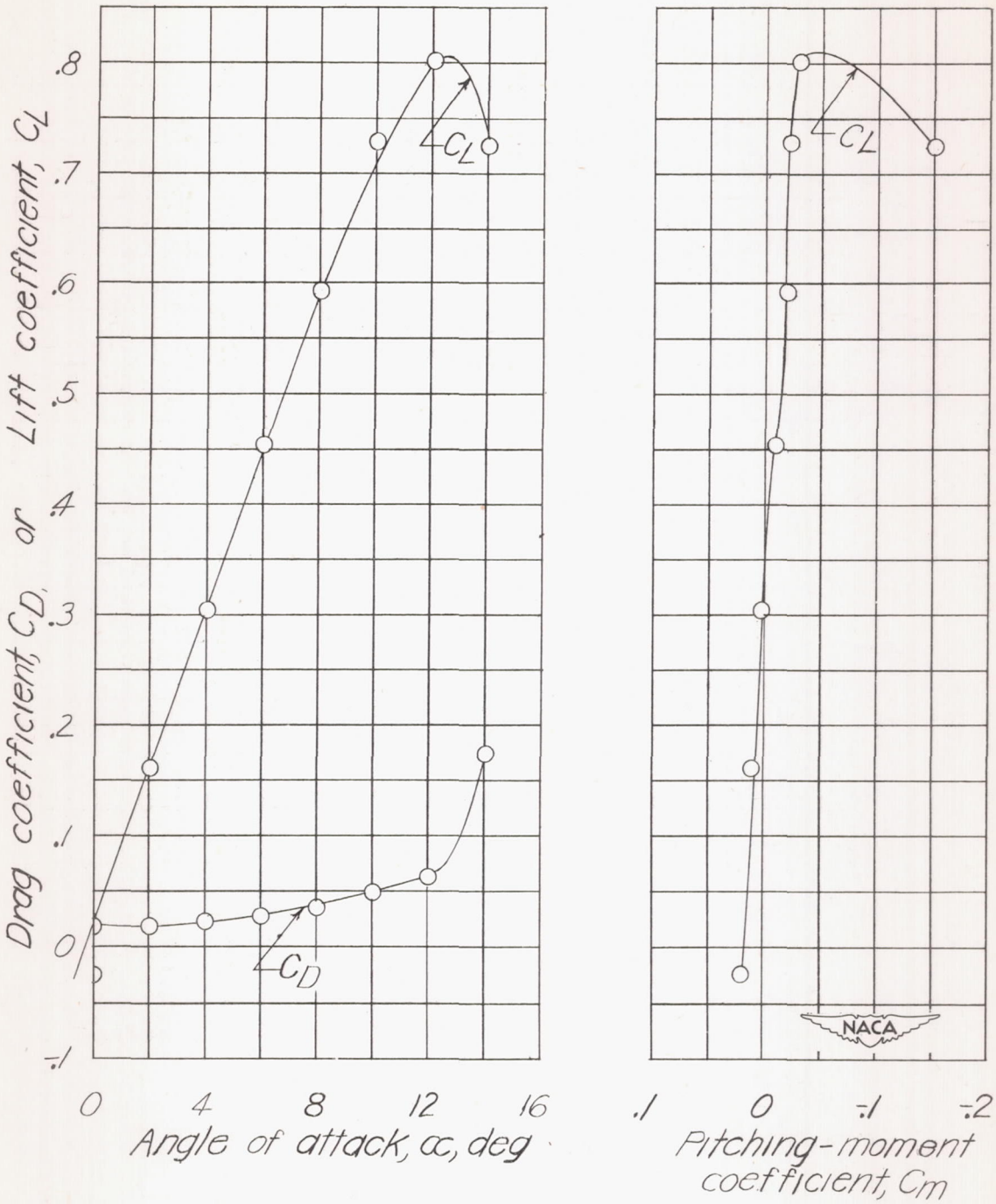

(a) Equivalent straight-wing model.

Figure 6.– Force tests of models.

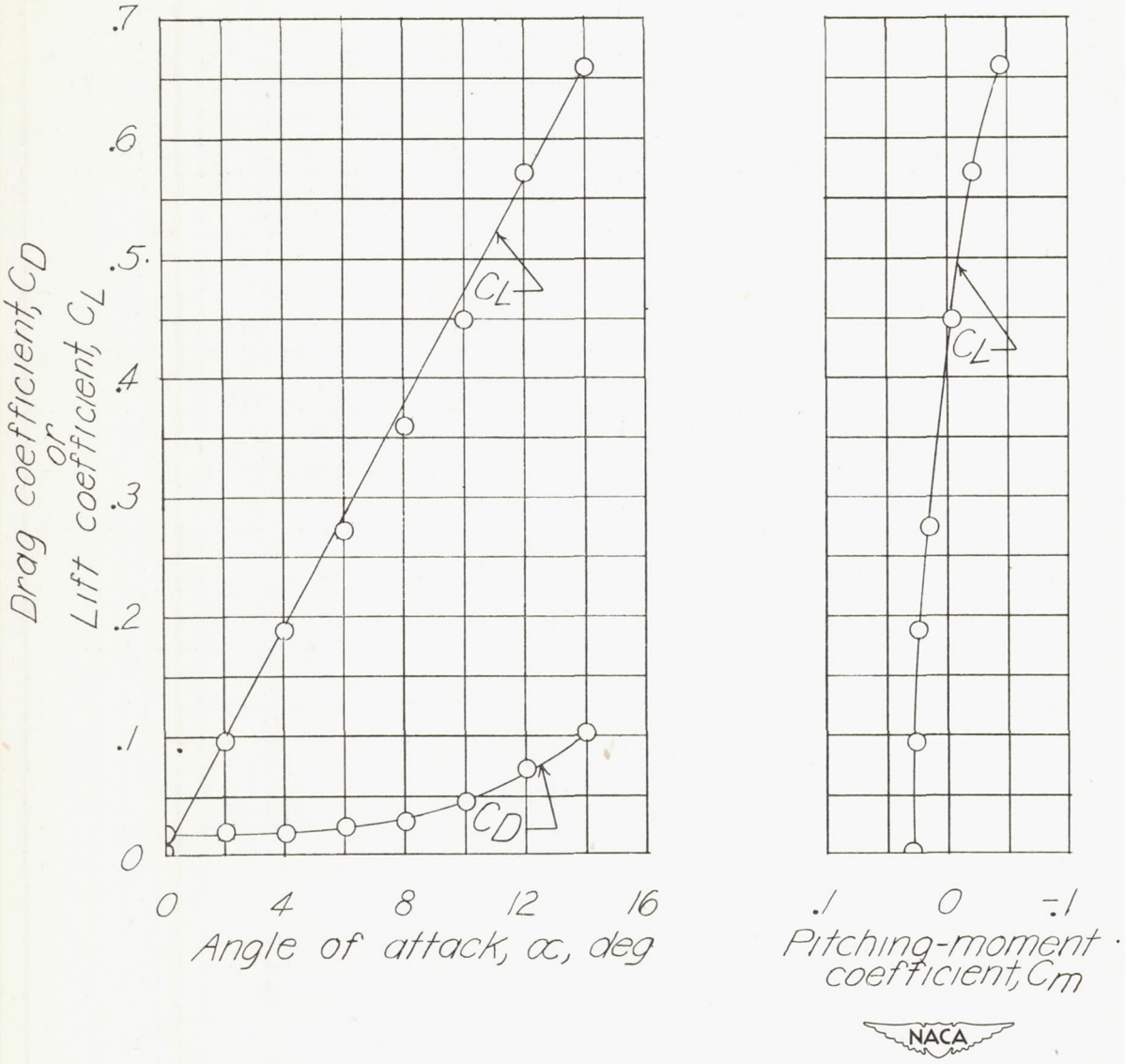

(b) 45° swept-back-wing model.

Figure 6.- Concluded.

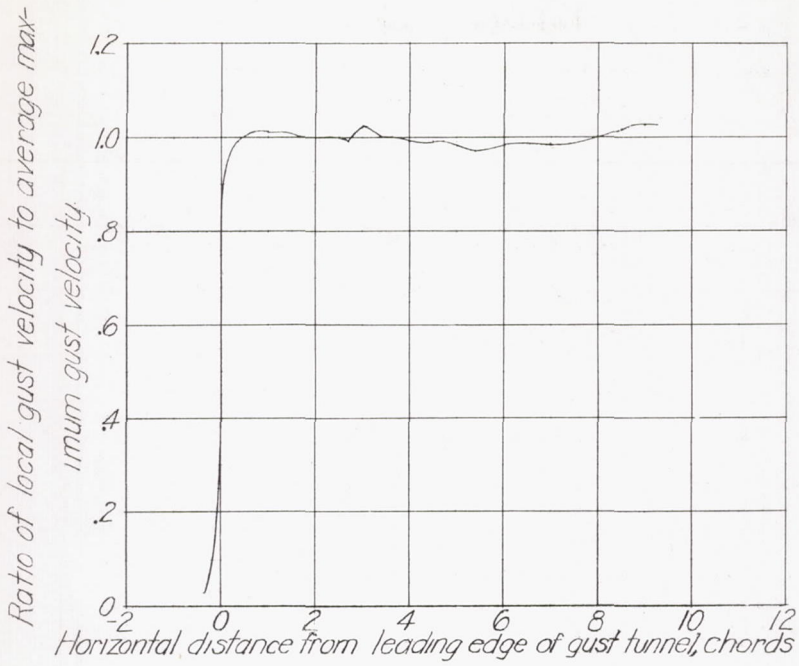

(a) 45° sweptback-wing model.

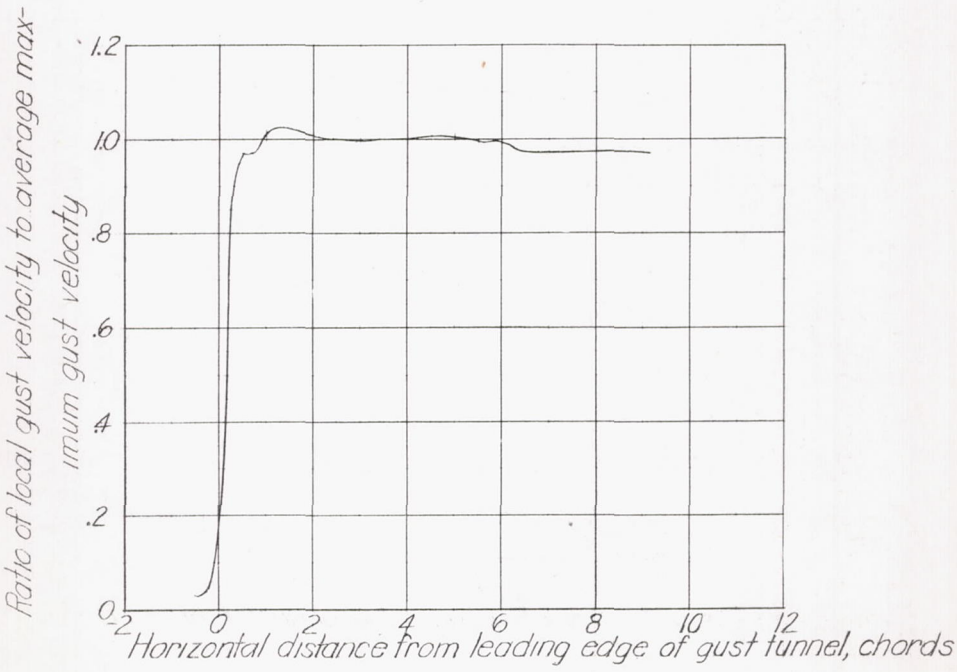

(b) Equivalent straight-wing model.

Figure 7.- Velocity distribution through jet.

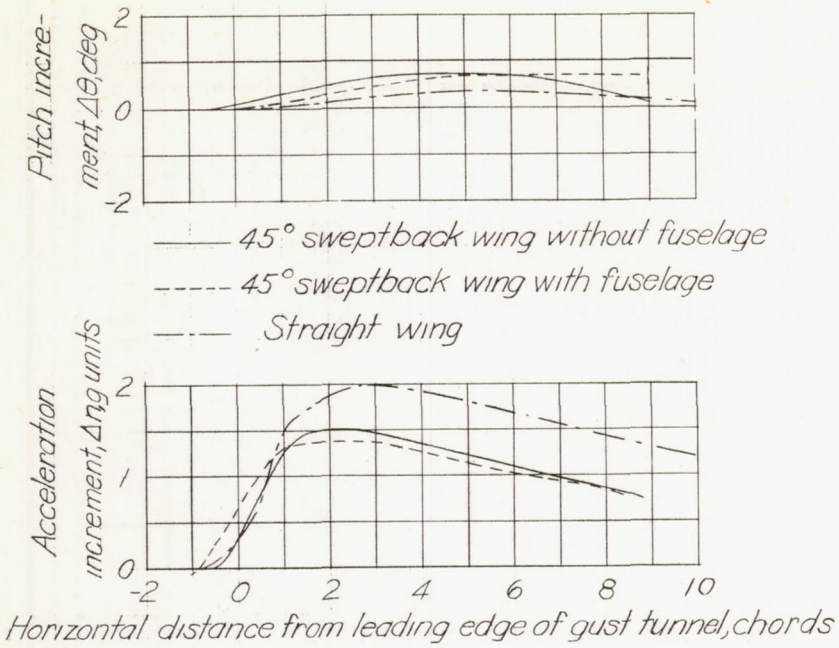

(a) Sharp-edge gust.

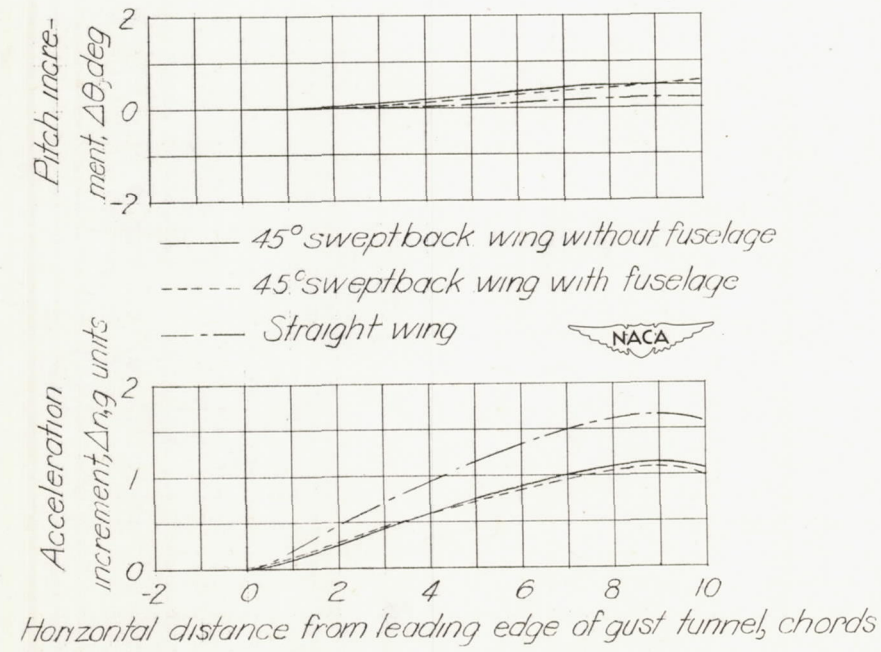

(b) Gust with 9-chord gradient distance. (Computed from experimental data for sharp-edge gust.)

Figure 8.– History of events in test gusts.

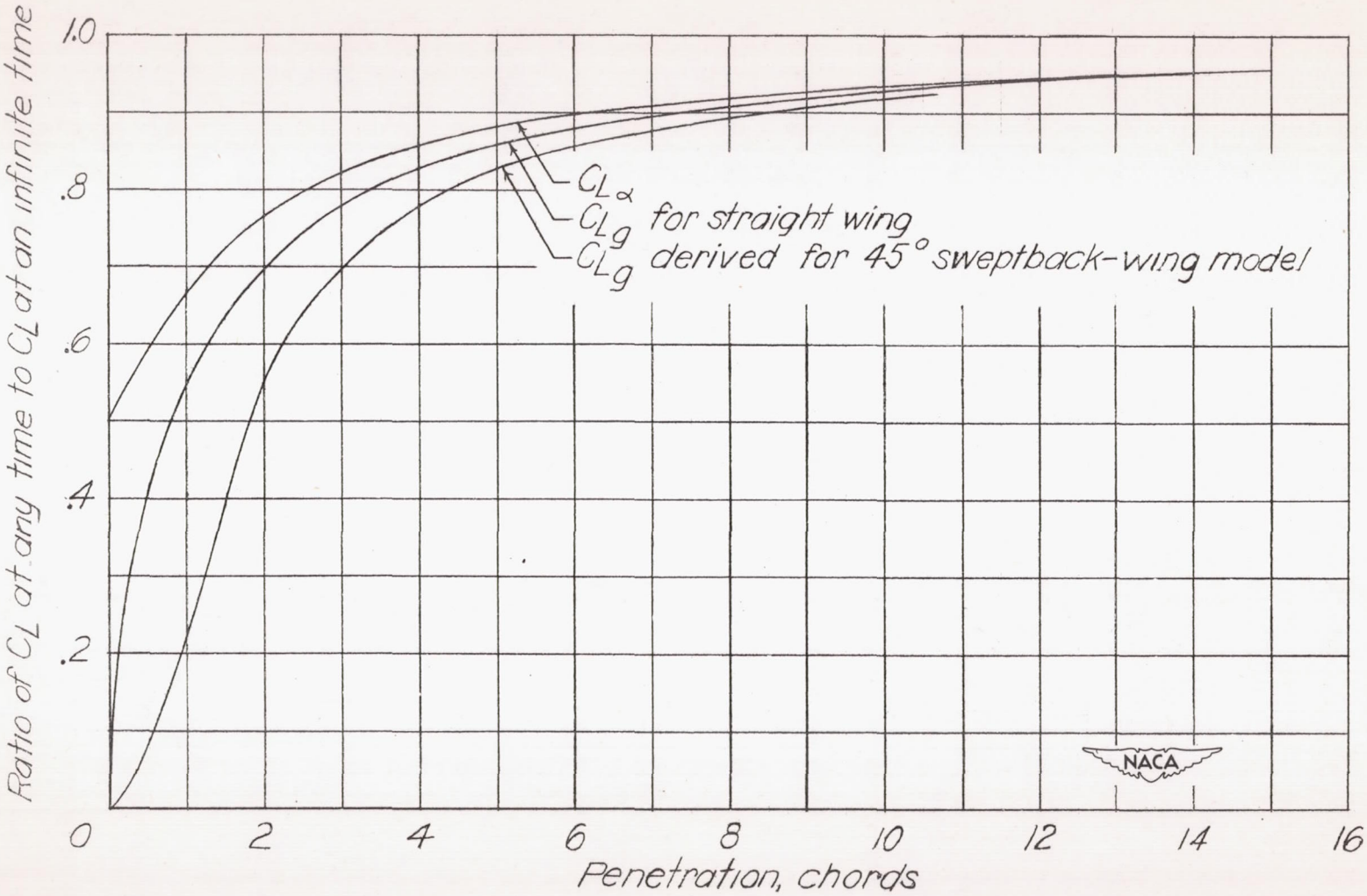

Figure 9.-Curves of C_{L_g} and C_{L_α} for infinite aspect ratio based on Jones' unsteady-lift functions (reference 5).